Steel and Composite Structures, *Vol. 31, No. 2 (2019) 113-123*
DOI: https://doi.org/10.12989/scs.2019.31.2.113

Mode-I fracture toughness of carbon fiber/epoxy composites interleaved by aramid nonwoven veils

Bertan Beylergil [*1,2], Metin Tanoğlu [2a] and Engin Aktaş [3b]

[1] *Department of Mechanical Engineering, Alanya Alaaddin Keykubat University, Alanya, Antalya, Turkey*
[2] *Department of Mechanical Engineering, Izmir Institute of Technology, Urla, İzmir, Turkey*
[3] *Department of Civil Engineering, Izmir Institute of Technology, Urla, İzmir, Turkey*

(*Received February 4, 2018, Revised March 12, 2019, Accepted March 22, 2019*)

Abstract. In this study, carbon fiber/epoxy (CF/EP) composites were interleaved with aramid nonwoven veils with an areal weight density of 8.5 g/m^2 to improve their Mode-I fracture toughness. The control and aramid interleaved CF/EP composite laminates were manufactured by VARTM in a [0]4 configuration. Tensile, three-point bending, compression, interlaminar shear, Charpy impact and Mode-I (DCB) fracture toughness values were determined to evaluate the effects of aramid nonwoven fabrics on the mechanical performance of the CF/EP composites. Thermomechanical behavior of the specimens was investigated by Dynamic Mechanical Analysis (DMA). The results showed that the propagation Mode-I fracture toughness values of CF/EP composites can be significantly improved (by about 72%) using aramid nonwoven fabrics. It was found that the main extrinsic toughening mechanism is aramid microfiber bridging acting behind the crack-tip. The incorporation of these nonwovens also increased interlaminar shear and Charpy impact strength by 10 and 16.5%, respectively. Moreover, it was revealed that the damping ability of the composites increased with the incorporation of aramid nonwoven fabrics in the interlaminar region of composites. On the other hand, they caused a reduction in in-plane mechanical properties due to the reduced carbon fiber volume fraction, increased thickness and void formation in the composites.

Keywords: composite structures; crack; fiber reinforced polymers (FRPs); fracture/fracture criteria; delamination; bending and shear strength; axial compression

1. Introduction

Carbon fiber/epoxy (CF/EP) composites are versatile engineering materials and they have been extensively used in aerospace and automotive industries where structural components are required to be light and highly durable. They have many unique advantages such as high strength and stiffness at low weight, good corrosion resistance, fatigue properties, tailor-ability and thermal properties. Today, more than 50% of the primary structure in Boeing 787 has been made of composite materials such as carbon fibers or sandwich panels (Kharazan *et al*. 2014, Pekbey *et al*. 2017, Ansari and Chakrabarti 2016, Fallah *et al*. 2018, Ho-Huu *et al*. 2018).

CF/EP composites are susceptible to delamination damage during the service life. Delamination, a frequently encountered mode of internal damage, may occur due to low-velocity impact events, manufacturing imperfections and stress concentrations triggered by sudden changes in structural details. This failure mode may reduce the in-plane stiffness and strength which results in accelerated growth of damage and premature failure. Also, CF/EP composites suffer low damping characteristics which result in reduced performance and life cycle, structural damage, annoying noise and discomfort. Therefore, delamination resistance and damping ability of these materials needs to be improved for promoting their widespread acceptance in the aerospace, automotive and wind-energy industries (Greenhalgh 2009, Greenhalgh *et al*. 2009, Mahieddine *et al*. 2015, Mohammadimehr *et al*. 2018, Liu and Shu 2015, Achache *et al*. 2017, Lakshmipathi and Vasudevan 2019).

The focus of various researchers has been the improvement of the delamination resistance of high-performance fiber reinforced composites. In general, two different approaches reported for preventing delamination failure in these composites; (i) mechanical approach and (ii) material approach. Mechanical approach includes weaving, stitching, z-pinning and braiding. This approach was shown to be very successful in improving damage tolerance of fiber-reinforced composites. For instance, interlaminar fracture toughness (IFT) can be enhanced by 20-50 times via stitching. Although Z-anchoring is only applicable for prepreg laminates, it increases IFT significantly (up to 470%). On the other hand, these modifications cause significant reductions in in-plane mechanical properties of the composites (Kuwata 2010). Steeves and Fleck (1999) showed that the presence of z-pins reduced the tensile and compressive strength of the composites by 37 and 30%, respectively. Reeder (1995) revealed that the tensile strength of the composites decreased about 30% reduction after stitching operation. Also, Kang and Lee (1994)

*Corresponding author, Ph.D.,
E-mail: bertan.beylergil@alanya.edu.tr
[a] Ph.D.
[b] Ph.D.

Copyright © 2019 Techno-Press, Ltd.

ISSN: 1229-9367 (Print), 1598-6233 (Online)

showed that increasing density of stitching for higher delamination resistance reduced tensile strength and modulus of the composites by 45 and 30%, respectively. It was also shown that the in-plane tension, compression and flexural properties of the 3D woven composites made by weaving or braiding were 10 to 45% lower than those of the control composites (Tanzawa *et al*. 2001, Brandt *et al*. 1996). In material approach, different types of micro or nano-sized fillers such as alumina, silica, carbon black, graphene, carbon nanotubes (CNTs) were mixed/stirred/ onicated with the matrix phase for improving delamination resistance. The increase in IFT achieved by filler addition can be in the range between 15-100% depending on the filler type and its content in the resin.

Recently, interleaving technique, based on insertion of an interleaf material at the interlaminar region, has been developed by some researchers. Various interleaf materials (micro or nano) such as thermoplastic and thermoset films, non-woven veils and self-same resin interleaf materials have been studied. In microfiber interleaving technique, interleaf material does not increase the uncured resin viscosity and the veil fibers are almost uniformly distributed in the resulting laminate as compared to filler toughening. The use of toxic and/or harmful, and also expensive fillers such as CNTs and graphene is not necessary. Also, the initial investment and maintenance cost of industrial textile machines used for weaving and stitching is not an issue in this technique which leads to significant financial savings. Recent studies on the effects of various micro nonwovens on the delamination resistance of laminated composites were summarized in the following paragraph.

Saz-Orozco *et al*. (2017) investigated the effects of polyamide (PA) and polyethylene terephthalate (PET) veils on the interlaminar fracture toughness (IFT) of a glass fiber/ vinyl ester (GF/VE) composites. The authors showed that PET veils have no significant effect on the IFT of composites while PA veils increased the mode I interlaminar fracture toughness values at crack initiation and propagation levels improved by 59 and 90%, respectively. Fitzmaurice *et al*. (2016) also showed that PET veils were not effective for improving Mode-I interlaminar fracture toughness of the glass fiber/ polyester resin (GF/PE) composites due to the weaker glass/resin interface providing an alternative crack propagation path. They also showed that the incorporation of PET veils had positive effects on the flexural strength, interlaminar shear strength and damping properties of the composites. Miller *et al*. (2015) observed a 40% increase in G_{Ic} with the addition of polyurethane (PU) veil. Ni *et al*. (2015) investigated the effects of aramid nonwoven veils on the mechanical properties of CF/bismaleimide (BMI) composites. Mode I interlaminar fracture toughness (G_{Ic}), Mode II interlaminar fracture toughness (G_{IIC}) and interlaminar shear strength of CF/BMI composites were also improved by 38.6, 15.5 and 10.2 %, respectively with the incorporation of aramid nonwoven veils. Ramirez *et al*. (2015) investigated the effects of polyether ether ketone (PEEK) and polyphenylene sulfide (PPS) interleaf materials on the delamination resistance of CF/EP composites. They showed that PEEK and PPS were promising interleaf materials for improving fracture toughness of these composites significantly. Lee *et al*. (2002) investigated the effects of carbon nonwoven veils on the Mode-I fracture toughness under different temperatures. They concluded that the Mode-I fracture toughness was not significantly affected with the incorporation of carbon nonwovens under room temperature.

In nanofiber interleaving technique, thermoplastic electrospun nanofibers are directly deposited onto dry/ pre-impregnated reinforcement fabrics. With this technique, it is possible to improve delamination resistance (fracture toughness) of CF/EP composites without negatively affecting their mechanical and thermomechanical properties (tensile and flexural modulus, glass transition temperature (T_g) and dynamic modulus etc.) unlike the other toughening methods. A recent review by Palazzetti and Zucchelli (2017) systematically reviewed the experimental studies of this topic. In the literature, different types of nanofibers such as PCL (Zhang *et al*. 2012), PVA (Beylergil *et al*. 2016), PU/CNTs (Liu *et al*. 2014), PSF (Li *et al*. 2008), and PA 66 (Beylergil *et al*. 2017, Beckermann and Pickering 2015) were used as secondary reinforcement between the primary reinforcing plies to improve both Mode-I and Mode-II fracture toughness of CF/EP and E-glass/epoxy laminated composites.

Although a few studies exist in the literature on the effects of aramid nonwoven fabrics on the Mode-I fracture toughness of fiber reinforced composites, further research is needed to clarify the effects of these nonwoven fabrics on the other in-plane mechanical properties of those composites.

In this study, CF/EP composites were interleaved with commercial aramid nonwoven fabrics to improve their Mode-I fracture toughness. The effects of aramid nonwoven fabrics on the in-plane mechanical properties of CF/EP composites were also evaluated. Thermomechanical behavior of the composites was determined via dynamic mechanic analysis (DMA). A series of mechanical tests such as Mode-I (DCB, double cantilever beam) fracture toughness, tensile, flexural, compression, interlaminar shear strength (ILSS) and Charpy-impact tests were carried out on the control and aramid interleaved composite specimens to reveal the potential use of aramid nonwoven interleaving system for composite structures.

2. Experimental

2.1 Materials

Unidirectional carbon fabrics with a fiber areal weight of 350 g/m^2 (Kordsa Global Inc. of Turkey) were used as the reinforcement material. The epoxy resin (Momentive^{TM} L160) and its hardener (Momentive^{TM} H160) were used with the weight ratio of 80:20, respectively. Commercial aramid nonwoven fabrics with 8.5 g/m^2 areal weight density were supplied from ACP Composites Inc., USA.

Table 1 shows some physical and mechanical properties of the aramid veils given by the manufacturer. SEM images of the aramid veils are shown in Fig. 1. The average fiber

diameter distribution was determined by measuring at least 25 fibers per sample using ImageJ software (National Institute of Mental Health, Bethesda, MD, USA). The average fiber diameter was determined as 15.36 ± 3.67 μm.

2.2 Manufacturing of composite test specimens

The control and aramid nonwoven interleaved composite laminates were fabricated by vacuum-infusion technique with a $[0]_4$ fiber orientation. Fig. 2 shows schematic representation of the control and aramid nonwoven interleaved composite laminates. For DCB laminates, only one aramid veil was placed between second and third plies before resin infusion. A polyimide film (Kapton®, 25 μm thick) was inserted in the middle of the plies to form an initial crack along the interlaminar region of the DCB specimens.

To determine other mechanical properties, aramid interleaved composite laminates were manufactured by placing one aramid veil between each carbon fabric before resin infusion. The composite laminates with/without aramid nonwoven veils were manufactured in the same vacuum bag in order to get more consistent test results and observe the effects of these veils on the resin flow during vacuum infusion. Based on the visual observations, no change of the resin flow was detected due to the aramid veils. Demolding of the manufactured composites was carried out after complete curing at room temperature, followed by a post curing in an oven at 80°C for 12 h.

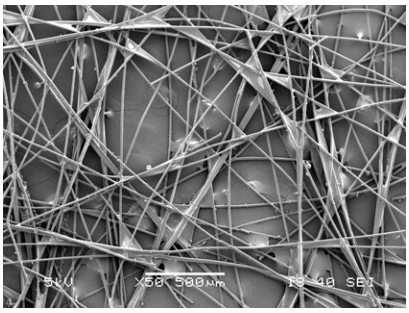

(a) 50x

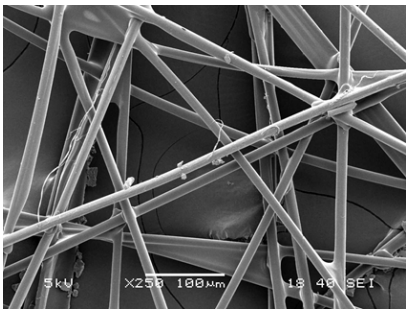

(b) 250x

Fig. 1 SEM images of aramid nonwoven veils

Table 1 Physical and mechanical properties of the aramid nonwoven veils

Fiber type	Binder	Average tensile strength (lb/in.) MD*	Average tensile strength (lb/in.) CD**	Area density (g/m^2)	Thickness (in.)
Kevlar29	Polyester	3.0	3.0	8.5	0.025

*MD: machine direction; **CD: cross direction

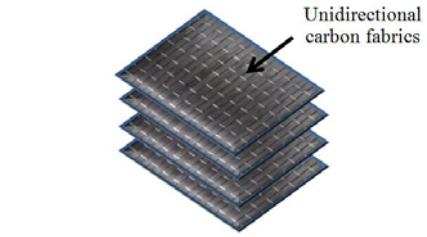

(a) Control

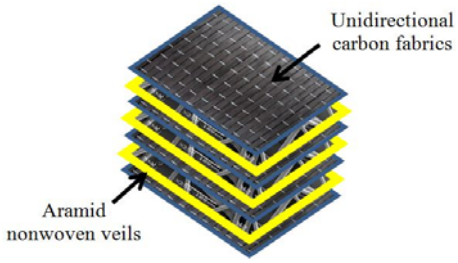

(b) Aramid interleaved

Fig. 2 Schematic representation of the composite laminates

Table 2 Fiber volume fraction (V_f) and average thickness of the composite laminates

Specimen	Veils in composite (%, wrt. carbon fabric weight)	Average thickness (mm)	Fiber volume fraction (V_f)
Control composite	-	1.25	0.55 ± 0.024
Aramid interleaved composite	1.82	1.44	0.49 ± 0.035

The fabricated composites were cut into desired dimensions using abrasive water-jet system. The fiber volume fraction (V_f) of the specimens was calculated by the Archimedes' Principle. Table 2 shows the resulting laminate thickness and calculated fiber volume fraction of the specimens. The thickness of the specimens (h) was measured as 1.25 and 1.44 mm for the control and aramid interleaved specimens, respectively. The increase in composite thickness due to aramid veils was 15.2%. However, the incorporation of 8.5 g/m^2 aramid veil caused no significant weight increase (about 1.82%) considering the weight of the carbon fabric (350 g/m^2). Their incorporation also resulted in a decrease of about 11% in the fiber volume fraction of the specimens.

2.3 Mechanical testing

All mechanical tests were performed at ambient conditions in accordance with the relevant ASTM standards.

(a)

(b)

(c)

Fig. 3 Photographs of the test specimens under (a) tensile; (b) compression; and (c) flexural loading

At least five iterations were tested as recommended in the ASTM standards. A universal testing machine with a 100 kN load capacity was used for the tensile, bending, compression, ILSS testing. The tensile tests (ASTM D3039) were carried out at a constant crosshead speed of 2.0 mm/min up to failure. A clip-on extensometer with knife edges was used to measure the strain (Fig. 3(a)) The compressive strength and modulus of the specimens were determined in accordance with ASTM D3410 standard. The dimensions of the compression test specimens were 140 mm in length and 12.7 mm in width. The gauge length was 12.7 mm. The specimens were placed in an anti-buckling fixture and loaded until failure at a constant crosshead speed of 1.3 mm/min (Fig. 3(b)). The flexural properties of the control and aramid interleaved specimens were obtained in accordance with ASTM D790 (Fig. 3(c)). A span-to-thickness ratio of 32 : 1 was used on the test fixture. The rate of crosshead motion was calculated for each group of specimens as recommended in the standard.

The interlaminar shear strength (ILSS) tests were determined based on the short beam shear configuration in accordance with ASTM D2344 standard. A span-to-thickness ratio of 4:1 was used with a span of 10 mm on the test fixture. The test speed was 1 mm/min. Charpy impact tests were carried out according to ISO-179 standard on 10 mm × 80 mm rectangular notched specimens, using the CEAST® Resil Impactor having maximum hammer energy of 15 J and hammer tangential speed of 3.46 m/s. At least ten specimens were tested for each group to obtain consistent average and standard deviation values.

The Mode-I interlaminar fracture toughness of the composites was determined by double cantilever beam (DCB) experiments. Shimadzu AGS-X testing machine mounted with a 5 kN load-cell was used for DCB experiments. The configuration of the specimens for DCB testing was shown in Fig. 4. The dimensions of the DCB test specimens were L = 150 mm in length and b = 25 mm in width. Aluminum blocks were bonded to outer surfaces of the DCB specimens to transfer the opening loads. Each specimen was initially loaded with a crosshead speed of 1 mm/min and the crack was allowed to propagate a short distance (3–5 mm) before the specimen was unloaded. The specimens were loaded until the crack propagates about 50-60 mm from tip of the crack. Load, opening displacement and crack length were recorded for the energy release rate (GI) calculation during the tests. G_I was calculated from Modified Beam Theory data reduction method given as follows (ASTM D5528)

$$G_I = \frac{F}{N}\frac{3P\delta}{2b\left(a+|\Delta|\right)} \tag{1}$$

where G_I is the Mode I interlaminar fracture toughness, P is the applied load, δ is the crosshead displacement, b is the specimen width, a is the delamination length (crack length), Δ is a value that is determined experimentally by generating a least squares plot of the cube root of compliance ($C^{1/3}$) as a function of delamination length. F and N are the

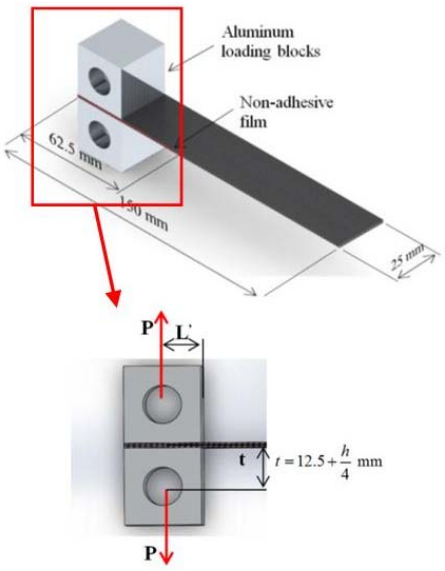

Fig. 4 Schematic representation of the DCB test specimens (ASTM D5528)

correction parameters to consider large displacement and the stiffening of the specimens by loading blocks, respectively. These correction factors can be calculated by using the following equations (ASTM D5528)

$$F = 1 - \left(\frac{3}{10}\right)\left(\frac{\delta}{a}\right)^2 - \left(\frac{3}{2}\right)\left(\frac{\delta t}{a^2}\right) \quad (2)$$

$$N = 1 - \left(\frac{L'}{a}\right)^3 - \left(\frac{9}{8}\right)\left[1 - \left(\frac{L'}{a}\right)^2\right]\left(\frac{\delta t}{a^2}\right) - \frac{9}{35}\left(\frac{\delta}{a}\right)^2 \quad (3)$$

where t and L' are illustrated in Fig. 4.

DMA tests were performed on the composite specimens using a DMA Q800 in a dual cantilever mode. The dimensions of the composite specimens were 65 mm in length and 10 mm in width. The heating rate was 20°C/min from room temperature to 150°C, and the frequency was 1 Hz. The storage modulus, loss modulus, and tan δ of the control and aramid interleaved composite specimens were calculated.

3. Results and discussion

Fig. 5 shows the typical load-displacement curves of the composite specimens (control and aramid interleaved) under tensile loading. The tensile stiffness and strength of the aramid interleaved composite specimens were found to be lower than the control specimens. The elastic modulus and tensile strength of the control composites were determined as 122.2 ± 3.4 GPa and 1792.0 ± 96 MPa, respectively. The incorporation of aramid nonwovens in the interlaminar region reduced the elastic modulus of the composites around 122 GPa to 115 GPa. Also, the tensile strength decreased from 1792 to 1560 MPa with the addition of aramid nonwoven fabrics. The reduction in elastic modulus and tensile strength were 6 and 13%, respectively. The reduction associates with reduced carbon fiber volume fraction due to increased thickness in the composites. Also, the void formation formed in the interleaved composites is related with the reduction in the tensile properties (Fig. 6). It is also noteworthy that the failure strain values of aramid-interleaved specimens are higher than those for the control specimens. The addition of aramid nonwovens in the interlaminar region resulted in more ductile response with respect to the control specimens.

Typical stress-strain curves of the composite specimens under flexural loading are shown in Fig. 7. As can be seen, the response of both specimens was almost similar at the initial part of the curves, although they exhibit a slight difference on the slope of the curves. However, failure modes of the specimens vary with the addition of interleaves. In the control specimens, the stress level reached to its maximum followed with a catastrophic failure. On the other hand, the incorporation of aramid nonwoven fabrics in the interlaminar region changed failure behavior so that the stress values started to decrease gradually after the maximum stress level was reached. Moreover, the strain values of aramid interleaved specimens were found to be much higher than those of the control specimens.

The addition of aramid nonwoven fabrics altered the failure mode from catastrophic to non-catastrophic nature which was also observed visually during the tests. The flexural modulus of the control and aramid interleaved composite specimens were determined as 105 ± 3.9, 87 ± 5.9 GPa, respectively. The addition of aramid nonwoven fabrics caused a reduction in the flexural modulus by about 18%. The flexural strength of the control and aramid interleaved composite specimens were determined as 1280 ± 90.8, 1100 ± 62.7 MPa, respectively. The reduction in flexural strength was about 14% as compared to control specimens. This can be attributed to the reduced carbon

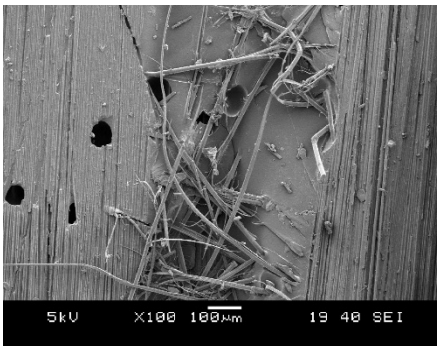

Fig. 6 Void formation observed in the aramid interleaved CF/EP composite specimens

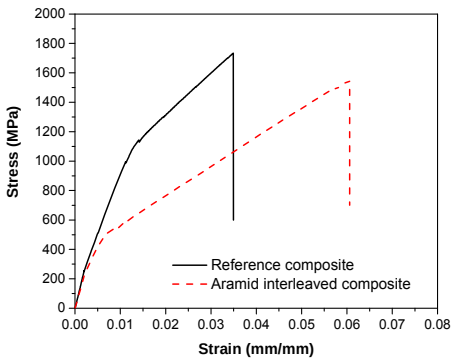

Fig. 5 Typical stress-strain curves of the CF/EP composite specimens under tensile loading

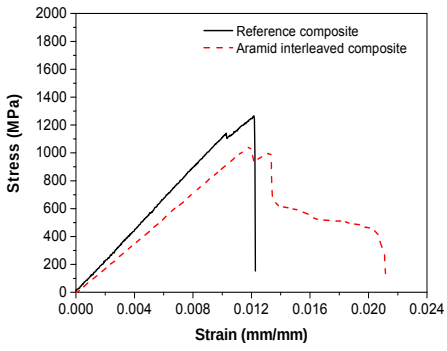

Fig. 7 Typical stress-strain curves of the CF/EP composite specimens under flexural loading

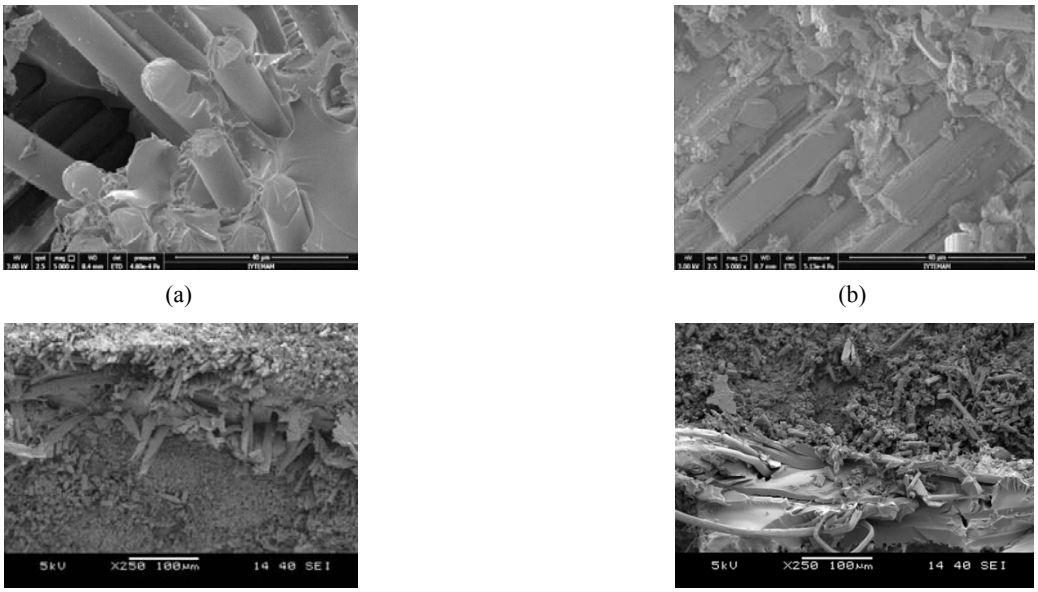

(a) (b)

(c) (d)

Fig. 8 SEM images of Charpy-impact (a)-(b) control and (c)-(d) aramid interleaved CF/EP composite specimens

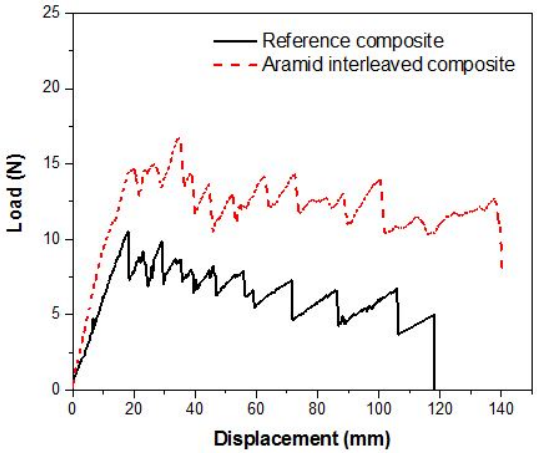

Fig. 7 Typical stress-strain curves of the CF/EP composite specimens under flexural loading

fiber volume fraction and increased thickness caused by the aramid nonwovens.

The compressive modulus and strength of the control specimens were determined as 113 GPa and 765 MPa, respectively. It was observed that the compressive strength and modulus decreased with the addition of aramid nonwoven fabrics. The compressive modulus and strength of the aramid interleaved composite specimens were determined as 88 GPa and 690 MPa, respectively. It was observed that the compressive modulus and strength of the composites were decreased about 23 and 10% respectively. This is due to the lower carbon fiber volume fraction and increased thickness compared to the control specimens. The impact fracture energy of the control specimens was measured to be 79.0 ± 5.5 kJ/m^2. The impact fracture energy increased about 16.5% (92.0 ± 6.6 kJ/m^2) by introducing aramid nonwoven veils on the interface area of composite laminates.

The improved impact energy can be explained by analyzing the SEM images of the fracture surfaces of control and aramid nonwoven interleaved specimens. As seen in Figs. 8(a)-(b), control specimens exhibited a glassy and smooth fractured surface and showed no sign of deformation. These are main characteristics of poor interfacial bonding. On the other hand, as seen in Figs. 8(c)-(d), aramid interleaved composite specimens exhibited more complex fractured surface which indicates higher matrix deformation and absorbed impact energy. During the impact, the nonwoven involved in resisting to the applied stress and improved the load-bearing capacity of the composites due to contribution of extensive deformations. The failure of the aramid fibers in Figs. 8(c)-(d) shows higher energy absorption and extensive deformations by the aramid fibers and distribution to the surrounding matrix. The imprints of broken and torn aramid fibers can be seen in Fig. 8(d).

The interlaminar shear strength (ILSS), one of the important parameters in many structural applications, can be considered as a quality control parameter related to delamination resistance. Therefore, the enhancement of ILSS is very important for the long-term safety of fiber reinforced polymer composites. The results of ILSS tests provide valuable insight for the response of composite specimens under Mode-I loading. The ILSS of the control specimens was determined as 59 ± 3.0 MPa. On the other hand, the ILSS of the aramid interleaved composite specimens were determined as 64.4 ± 1.33 MPa. It was observed that the incorporation of aramid nonwoven veils led to increase about 10%. The improved shear performance may be related to good chemical bonding between aramid and epoxy matrix that improves the wetting efficiency and gives a resin-rich surface which possibly arrests the crack initiation at the interface of the composites. Also, the polymer matrix containing aramid microfibers led to a more uniform distribution of shear stresses in the interlaminar

region and transmitted the load to the carbon plies resulting in higher shear strength with a lower standard deviation. In aramid interleaved composite specimens, the ILSS failure was triggered by microfiber/epoxy debonding, instead of CF/epoxy debonding.

Fig. 9 shows the representative load-displacement curves of the composite specimens under Mode-I loading. The maximum load (P_{max}) values were determined as 11.83 ± 1.43 N and 13.76 ± 1.05 N for the control and aramid nonwoven fabric interleaved composite specimens, respectively. It was observed that the maximum force increased about 25% with the addition of aramid nonwovens as compared to control specimens. The fracture behavior of the control and aramid interleaved laminates was observed to be almost similar. The load-displacement curves of the specimens were jag-shaped which generally observed in the unidirectional carbon fiber reinforced composites. Although similar behavior was observed in both specimens, the crack in the control specimens jumped more extensively while the crack traveled much more slowly during the crack propagation for aramid interleaved composite specimens. More gradual load drop was observed in the aramid interleaved composite specimens at higher displacement values as can be seen in Fig. 9. The maximum displacement values were 121 ± 2.5 mm and 131 ± 11.2 mm for the control and aramid interleaved specimens, respectively.

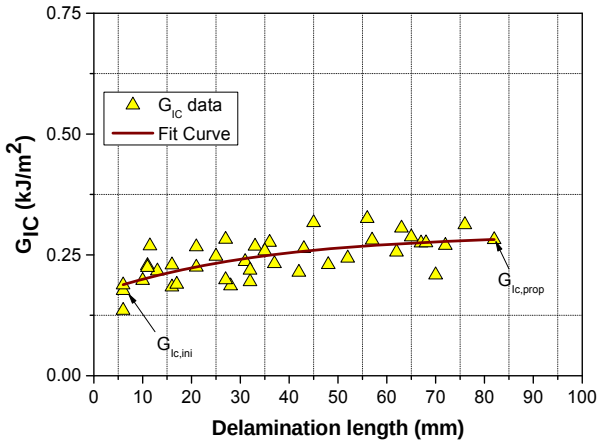

(a)

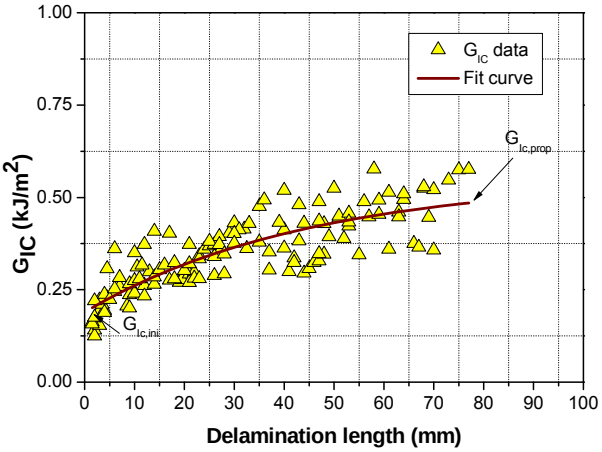

(b)

Fig. 10 R-curves of the (a) control; and (b) aramid interleaved CF/EP composite specimens (Curve fitting function: $y = y_0 + A \times e^{R_o x}$)

Table 3 Curve fitting parameters for control and aramid interleaved composites

Specimen	y_0	A	R_o
Control composite	0.29364	-0.12521	-0.02881
Aramid interleaved composite	0.55042	-0.36102	-0.02218

Fig. 10 shows the R-curves of the control and aramid veil interleaved DCB specimens. An exponential curve was fitted to the Mode-I fracture toughness data in order to determine the initiation and propagation fracture toughness values of the composites. Curve-fitting parameters were presented in Table 3. The initiation and propagation values of the control composite specimens were determined as 0.19 and 0.28 kJ/m^2, respectively. For the composites with aramid nonwoven fabrics, the initiation and propagation Mode-I fracture toughness values were determined as 0.20 and 0.48 kJ/m^2, respectively. It can be said that aramid nonwoven veils did not have a significant effect on the initiation Mode-I fracture toughness. The initiation Mode-I fracture toughness remained unchanged with the addition of aramid nonwoven veils. The maximum load and corresponding displacement values were not significantly changed until the first crack became visible from the crack tip. However, the effects of aramid nonwovens became more apparent as the crack was propagated.

The increasing tendency of G_{Ic} values with crack extension dictates the fiber bridging phenomenon in the aramid interleaved composite specimens. It was seen that the propagation Mode-I fracture toughness increased from 0.30 to 0.50 kJ/m^2. This corresponds to 72% increase in Mode-I fracture toughness values. The average Mode-I fracture toughness ($G_{Ic,ave}$) was increased from 0.23 kJ/m^2 to 0.34 kJ/m^2 with the incorporation of aramid nonwoven fabrics. The maximum G_{Ic} values were determined as 0.33 kJ/m^2 and 0.60 kJ/m^2 for the control and aramid interleaved specimens, respectively.

The SEM fracture surface images of the control Mode-I specimens are shown in Fig. 11. The micrographs were taken from the middle of the specimens (away from the initial crack region) for interpreting fracture mechanisms. As seen in Figs. 11(a)-(b), the control specimens exhibit smooth and featureless (indicating more brittle) failure characteristics of the composites under Mode-I loading. Mode-I fracture toughness is controlled by mechanisms such as cohesive fracture of the matrix and fiber bridging.

Debonding of the fibers from the polymer matrix is visible in Fig. 11(c). In the unidirectional CF/EP composites, the main toughening mechanisms are fiber bridging in the wake of the propagating crack tip. This mechanism increases the interlaminar resistance to delamination growth especially after the crack propagates about 30-40 mm away from the crack tip. The main fracture process observed for the control specimens was cohesive failure of the matrix. Fig. 11 also shows SEM images of the

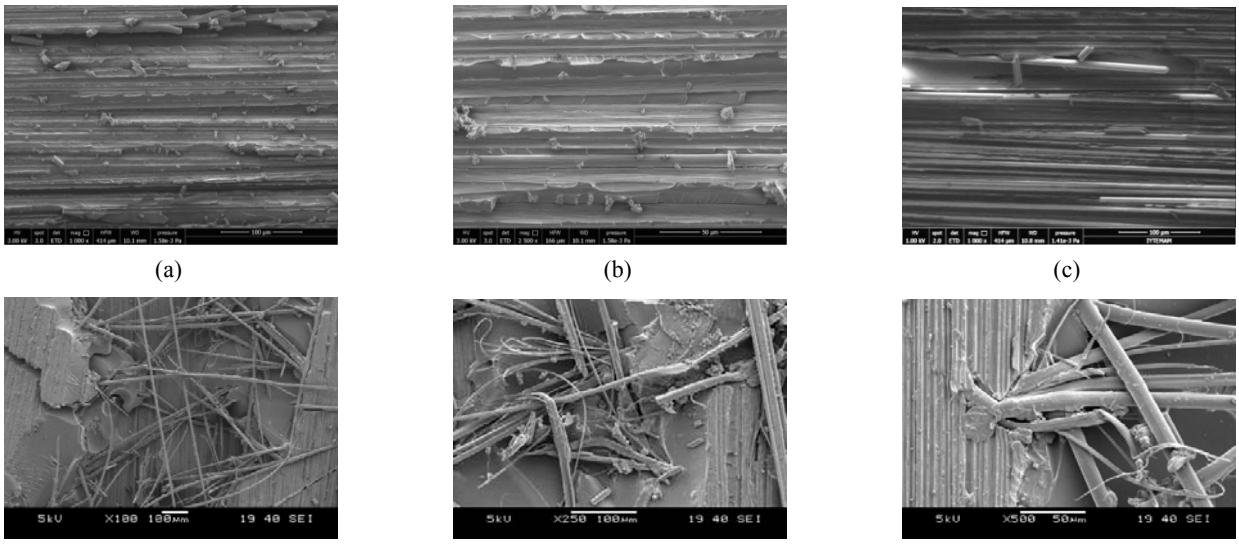

Fig. 11 SEM images of the fractured DCB specimens: (a), (b), (c) control; and (d), (e), (f) aramid interleaved CF/EP composite specimens

aramid interleaved specimens' fracture surfaces. It was note-worthy that aramid interleaved specimens exhibit a combination of smooth and deformed regions (deformation of the matrix material and aramid fibers) as seen in Figs. 11(d)-(e). The change from a smooth to rough fracture path proves the toughening effect of aramid fibers. Fig. 11(f) shows an example image of deformed aramid fibers within the matrix. Aramid fiber imprints within the matrix can be also seen in this figure. These figures support the hypothesis of more stable crack propagation in the composites with aramid nonwoven modification. The main toughening mechanism was crack bridging by aramid fibers as the crack continued to propagate. This toughening mechanism is one of the extrinsic types of toughening mechanisms which occurs behind the crack tip. Therefore, the initiation Mode-I fracture toughness was not influenced by the incorporation of aramid nonwovens as observed in the DCB tests. However, these nonwovens led to significant increase in propagation Mode-I fracture toughness values as compared to control specimens.

DMA test results of the composite specimens are presented in Table 4. The storage modulus is the elastic response of the material representing the elastic response and the loss modulus measures the energy dissipated as heat. The results showed that both storage modulus decreased with the incorporation of aramid nonwoven fabrics in the interlaminar region of the composites. The interleaf material gives more flexibility resulting in the low stiffness and low storage modulus. The decrease in storage modulus was about 20% as compared to control composite specimens. This result was also consistent with the three-point bending test results. The loss modulus of the composites exhibited a small increase with the addition of aramid nonwoven fabrics. Additionally, *tanδ* at room temperature and *tanδ* (*peak*) values increased about 27 and 33% respectively. Therefore, it can be concluded that the damping ability of the composites improved significantly with the addition of aramid nonwoven fabrics on the interlaminar region of composites. In Table 4, the glass transition temperature (T_g) of the specimens are also reported. The T_g of control composite specimens was determined as 97°C whereas the Tg of aramid nonwoven interleaved specimens were determined as 96°C. The T_g of all specimens were in the range between 95° and 96°C. It was observed that aramid interleaving system had no significant effect on the T_g of composite specimens. The good chemical interaction between the aramid fibers and epoxy resin retained the T_g of the composites. The DMA results indicated that although the aramid veils caused a decrease in the storage modulus of the specimens, the operating temperature of the composites, in which storage modulus was constant, was not affected due to the presence of aramid nonwoven fabrics.

A comparison of aramid interleaving system developed within the present study and the others reported in the literature is given in Table 5. As can be seen, our findings

Table 4 DMA test results of the composite specimens

Specimen	Storage modulus (GPa, 25°C)	Loss modulus (MPa, 25°C)	tanδ	tanδ (peak)	T_g (°C)	Specimen
Control composite	66005	955	0.0144	0.461	96.2	Control composite
Aramid interleaved composite	52902	965	0.0182	0.613	95.9	Aramid interleaved composite

are consistent with the results reported in the literature. The effectiveness of nonwoven interleaving system depends on the ability of fiber bridging of the nonwovens. Although aramid interleaves are less effective as compared to PA interleaves in terms of improvements in delamination resistance, aramid interleaves exhibited better performance than the other interleaf materials such as PU, PE and CF. As expected, fracture toughness increases with the increase of areal weight density. This due to the fact that the amount of bridging fibers increases with the increase of areal weight density. It was also seen that there was almost a linear relationship between areal weight density and toughness improvement for PA interleaving (Nash *et al*. 2016, O'Donovan *et al*. 2014).

Fig. 12 shows the change in the crack path for different interleaving systems. If the microfibers remain inside in the epoxy matrix and not pull-out from the matrix, the improvement in Mode-I fracture toughness was not significant. As an example, although carbon fibers were much stronger than the others, these fibers showed very small amount of fiber bridging and remained inside the epoxy matrix therefore no significant improvement was obtained in Mode-I fracture toughness. If the crack jumps to the relatively weak fiber/matrix interface instead of propagating in nonwoven/nonwoven interface (fiber bridging not occurs), the improvement is expected to be as low as observed in the case of CF interleaving.

Table 5 also shows the effects of nanofiber interleaf materials on the delamination resistance of laminated composites. As in the case of microfiber interleaving, most of the studies were focused on PA nanofiber interleaving in the literature. It is obvious that PA is the most promising material among the other polymers in terms of improvement in delamination resistance of laminated composites. It was noteworthy that nanofiber interleaving is more effective than microfiber interleaving. The delamination resistance of laminated composites could be improved significantly by using smaller amount of nanofibers in the interlaminar region as compared to microfiber interleaving. For instance, it was shown that the incorporation of PA 6,6 nanofibers with an areal density of 1.0 g/m^2 led to significant increase in Mode-I fracture toughness values of CF/EP composites about 50%. As in the case of microfiber interleaving, there is a linear relationship between the amount of nanofibers in the interlaminar region and fracture toughness improvement. Beckermann and Pickering (2015) showed that it was

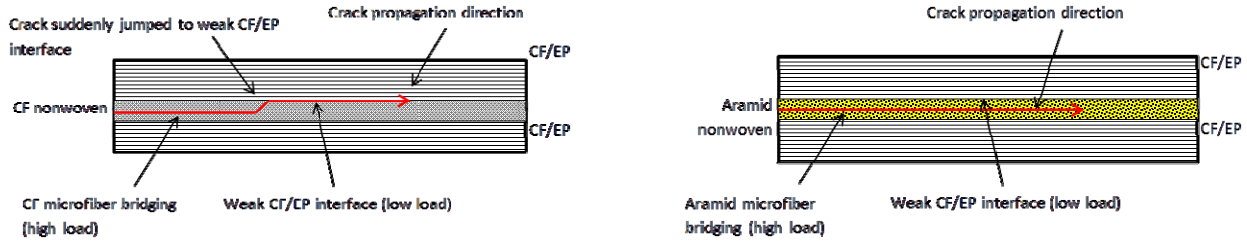

(a) (b)

Fig. 12 Schematic representation of the crack propagation in (a) CF and (b) aramid interleaved composite specimens

Table 5 A comparison of aramid interleaving system with the other micro/nano interleaving systems reported in the literature (m: micro interleaf material, n: nano interleaf material)

Reference	Composite system	Interleaf material	Areal weight density (g/m^2)	Mode-I fracture toughness (% increase)
Present study	CF/EP	m-AR	8.5	72
Kuwata 2010	CF/EP	m-PE	20	83
Saz-Orozco et *al*. (2017)	GF/VE	m-PA	17	90
Fitzmaurice et *al*. (2016)	GF/VE	m-PET	45	12
Miller et *al*. (2015)	GF/PE	m-PU	15	40
Ni et *al*. 2015	CF/BMI	m-AR	16	108
Lee et *al*. 2002	CF/EP	m-CF	12	28
Ramirez et *al*. 2015	CF/EP	m-PEEK	11	102
Ramirez et *al*. (2015)	CF/EP	m-PPS	40	133
Nash et *al*. (2016)	CF/ BE	m-PA	34	352
O'Donovan et *al*. (2014)	GF/PE	m-PA	17	170
Beckermann and Pickering 2015	CF/EP	n-PA	1.5	55
Beckermann and Pickering (2015)	CF/EP	n-PA	4.5	156
Beckermann and Pickering (2015)	CF/EP	n-PA	9.0	173
Beylergil et *al*. (2017)	CF/EP	n-PA	1.0	50

possible to improve fracture toughness about 55% by using PA nanofibers with an areal weight density of 1.5 g/m^2. The delamination resistance of composites was improved by 155% as the areal weight density was tripled. Then, the improvement in fracture toughness reached a plateau with the increase of nanofiber amount (9.0 g/m^2) in the interlaminar region.

It was also proven in the study by Molnar *et al*. (2014) that the incorporation of different polymeric nanofibers such as polyacrylonitrile (PAN) in the interlaminar region can be used to improve not only delamination resistance but also in-plane mechanical properties of composite laminates. The authors showed that the interlaminar shear strength of unidirectional CF/EP composites could be increased by 11%. Also, they showed that the flexural strength and modulus of these composites could be increased by 21 and 54%, respectively. Charpy impact test results showed that the energy to maximum force could be increased by 64% by incorporating PAN nanofibers in the interlaminar region of CF/EP composites. This win-win situation is the unique characteristic of nanofiber interleaving technique. Therefore, the nanofiber interleaving technique can be considered as the best solution for the delamination problem observed in the laminated composites. However, there are some issues that should be considered before commercialization step. For instance, the use of highly volatile and hazardous chemicals such as formic acid and chloroform is the critical issue that needs to be considered. Moreover, it is very difficult to produce electrospun nanofibers uniformly for a long period of time due to variation of polymer flow within the electrospinning nozzles. The possible variations in the nanofiber nonwoven thickness may lead to misjudge of experimental results.

4. Conclusions

In this study, aramid nonwoven fabrics were used as an interleaf material to improve Mode-I delamination resistance of CF/EP composites. A series of mechanical tests were carried to investigate the effects of aramid interleaving systems on the mechanical performance of CF/EP composites. The results showed that the steady state regime Mode-I fracture toughness of CF/EP composites could be improved about 72%, using aramid nonwovens. Additionally, the ILSS and Charpy impact strength could be increased about 10 and 16.5% respectively by the addition of aramid nonwovens. DMA results indicated that T_g was not affected whereas the damping ability of the CF/EP composites improved significantly by the incorporation of aramid nonwoven fabrics. On the other hand, these nonwoven fabrics reduced in-plane mechanical properties such as tensile, flexural and compressive strength due to the lower carbon fiber fraction, increased thickness and void formation in the resulting composite laminate. Aramid interleaving system can be used in structural applications subjected to out-of-plane loading in service for improved delamination resistance with minimal cost, and reduced health and safety issues. Aramid interleaves can be an optimum alternative to PEEK, PE, PET, PU and PPS interleaf materials. Additionally, instead of using in the whole composite structure, critical areas with high stress concentrations such as near holes, notches and sharp corners can be interleaved with aramid nonwoven fabrics for better delamination and impact resistance.

References

Achache, H., Benzerdjeb, A., Mehidi, A., Boutabout, B. and Ouinas, D. (2017), "Delamination of a composite laminated under monotonic loading", *Struct. Eng. Mech., Int. J.*, **63**(5), 597-605.

Ansari, Md. and Chakrabarti, A. (2016), "Behaviour of GFRP composite plate under ballistic impact: experimental and FE analyses", *Struct. Eng. Mech., Int. J.*, **60**(5), 829-849.

Beckermann, G. and Pickering, K. (2015), "Mode I and Mode II interlaminar fracture toughness of composite laminates interleaved with electrospun nanofibre veils", *Compos. Part A: Appl. Sci. Manuf.*, **72**, 11-21.

Beylergil, B., Tanoglu, M. and Aktas, A. (2016), "Modification of carbon fibre/epoxy composites by polyvinyl alcohol (PVA) based electrospun nanofibers", *Adv. Compos. Lett.*, **25**(3), 69-76.

Beylergil, B., Tanoglu, M. and Aktas, A. (2017), "Enhancement of interlaminar fracture toughness of carbon fiber-epoxy composites using polyamide-6,6 electrospun nanofibers", *J. Appl. Polym. Sci.*, **134**(35), 1-12.

Brandt, J., Drechsler, K. and Arendts, F.–J. (1996), "Mechanical performance of composites based on various three-dimensional woven-fibre performs", *Compos. Sci. Technol.*, **56**(3), 381-386.

Fallah, N., Vaez, S.R.H. and Fasihi, H. (2018), "Damage identification in laminated composite plates using a new multi-step approach", *Steel Compos. Struct., Int. J.*, **29**(1), 139-149.

Fitzmaurice, K., Ray, D. and McCarthy, M.A (2016), "PET interleaving veils for improved fracture toughness of glass fibre/low-styrene-emission unsaturated polyester resin composites", *J. Appl. Polym. Sci.*, **133**, 42877.

Greenhalgh, E.S. (2009), *Failure Analysis and Fractography of Polymer Composites*, (1st Edition), Woodhead Publishing Ltd., Elsevier, USA.

Greenhalgh, E.S., Rogers, C. and Robinson, P. (2009), "Fractographic observations on delamination growth and the subsequent migration through the laminate", *Compos. Sci. Technol.*, **69**(14), 2345-2351.

Ho-Huu, V., Vo-Duy, T., Duong-Gia, D. and Nguyen-Thoi, T. (2018), "An efficient procedure for lightweight optimal design of composite laminated beams, *Steel Compos. Struct., Int. J.*, **27**(3), 297-310.

Kang, T.J. and Lee, S.H. (1994), "Effect of stitching on the mechanical and impact properties of woven laminate composite", *J. Compos. Mater.*, **28**(16), 1574-1587.

Kharazan, M., Sadr, M.H. and Kiani, M. (2014), "Delamination growth analysis in composite laminates subjected to low velocity impact", *Steel Compos. Struct., Int. J.*, **17**(4), 387-403.

Kuwata, M. (2010), "Mechanisms of interlaminar fracture toughness using non-woven veils as interleaf materials", Ph.D. Dissertation; Queen Mary University, London, UK.

Lakshmipathi, J. and Vasudevan, R. (2019), "Dynamic characterization of a CNT reinforced hybrid uniform and non-uniform composite plates", *Steel Compos. Struct., Int. J.*, **30**(1), 31-46.

Lee, S.H., Noguchi, H., Kim, Y.B. and Cheong, S.K. (2002), "Effect of interleaved non-woven carbon tissue on interlaminar fracture toughness of laminated composites: Part I - Mode II", *J. Compos. Mater.*, **36**(18), 2153-2168.

Li, G., Li, P., Yu, Y., Jia, X., Zhang, S., Yong, X. and Ryu, S. (2008), "Novel carbon fiber/epoxy composite toughened by electrospun polysulfone nanofibers", *Matter*. *Lett*., **62**(3), 987-994.

Liu, Y. and Shu, D.W. (2015), "Effects of edge crack on the vibration characteristics of delaminated beams", *Steel Compos*. *Struct*., *Int*. *J*., **53**(4), 767-780.

Liu, L., Zhang, H. and Zhou, Y. (2014), "Quasi-static mechanical response and corresponding analytical model of laminates incorporating with nanoweb interlayers", *Compos*. *Struct*., **111**, 436-445.

Mahieddine, A., Ouali, M. and Mazouz, A. (2015), "Modeling and simulation of partially delaminated composite beams", *Steel Compos*. *Struct*., *Int*. *J*., **18**(5), 1119-1127.

Miller, S.G., Roberts, G.D., Kohlman, L.W., Heimann, P., Pereira, M., Rugreri, C. and Martin, R. (2015), "Impact behavior of composite fan blade leading edge subcomponent with thermoplastic polyurethane interleave", *Proceedings of 20th International Conference on Composite Materials*, Copenhagen, Denmark.

Mohammadimehr, M., Mohammadi-Dehabadi, A.A., Akhavan Alavi, S.M., Alambeigi, K., Bamdad, M., Yazdani, R. and Hanifehlou, S. (2018), "Bending, buckling, and free vibration analyses of carbon nanotube reinforced composite beams and experimental tensile test to obtain the mechanical properties of nanocomposite", *Steel Compos*. *Struct*., *Int*. *J*., **29**(3), 405-422.

Molnar, K., Kostakova, E. and Meszaros, L. (2014), "The effect of needleless electrospun nanofibrous interleaves on mechanical properties of carbon fabrics/epoxy laminates", *eXPRESS Polym Lett*., **8**(1), 256-262.

Nash, N.H., Young, T.M. and Stanley, W.F. (2016), "The reversibility of Mode-I and -II interlaminar fracture toughness after hydrothermal aging of Carbon/Benzoxazine composites with a thermoplastic toughening interlayer", *Compos*. *Struct*., **152**, 558-567.

Ni, N., Wen Y., He, D., Yi, X., Zhang, T. and Xu, Y. (2015), "High damping and high stiffness CFRP composites with aramid non-woven fabric interlayers", *Compos*. *Sci*. *Technol*., **117**, 92-99.

O'Donovan, K., Ray, D. and McCarthy, M.A. (2014), "Toughening Effects of Interleaved Nylon Veils on Glass Fabric/Low-Styrene-Emission Unsaturated Polyester Resin Composites", *J*. *Appl*. *Polym*. *Sci*., **132**, 41462.

Palazzetti, R. and Zucchelli, A. (2017), "Electrospun nanofibers as reinforcement for composite laminates materials-A review", *Compos*. *Struct*., **182**, 711-727.

Pekbey, Y., Aslantaş, K. and Yumak, N. (2017), "Ballistic impact response of Kevlar Composites with filled epoxy matrix", *Steel Compos*. *Struct*., *Int*. *J*., **24**(2), 191-200.

Ramirez, V.A., Hogg, P.J. and Sampson, W.W. (2015), "The influence of the nonwoven veil architectures on interlaminar fracture toughness of interleaved composites", *Compos*. *Sci*. *Technol*., **110**, 103-110.

Reeder, J.R. (1995), "Stitching vs. a toughened matrix: compression strength effects", *J*. *Compos*. *Mater*., **29**, 2464-2487.

Saz-Orozco, B.D., Ray, D. and Stanley, W.F. (2017), "Effect of thermoplastic veils on interlaminar fracture Toughness of a Glass Fiber/Vinyl Ester Composite", *Polym*. *Compos*., **38**(11), 2501-2508.

Steeves, C. and Fleck, N.A. (1999), "Z-pinned composite laminates: knockdown in compressive strength", *Proceedings of the 5th Conference of Delamination and Fracture of Composites*, London, UK, March, pp. 60-68.

Tanzawa, Y. Watanabe, N. and Ishikawa, T. (2001), "FEM simulation of a modified DCB test for 3-D orthogonal interlocked fabric composites", *Compos*. *Sci*. *Technol*., **61**(8), 1097-1107.

Zhang, J., Yang, T., Lin, T. and Wang, C-H. (2012), "Phase morphology of nanofibre interlayers: Critical factor for toughening carbon/epoxy composites", *Compos*. *Sci*. *Technol*., **72**(2), 256-262.

CC